The Abdus Salam International Centre for Theoretical Physics

United Nations Educational, Scientific and Cultural Organization

IAEA International Atomic Energy Agency

1965-5

9th Workshop on Three-Dimensional Modelling of Seismic Waves Generation, Propagation and their Inversion

22 September - 4 October, 2008

Inverse problem

Structural models of the lithosphere-asthenosphere system in the Mediterranean: seismic and volcanic activity

G.F. Panza

Dept. of Earth Sciences/ICTP, Trieste

panza@dst.units.it

Inverse problem

Structural models of the lithosphere-asthenosphere system in the Mediterranean: seismic and volcanic activity

Giuliano F. Panza

Trieste 22 September - 4 October 2008

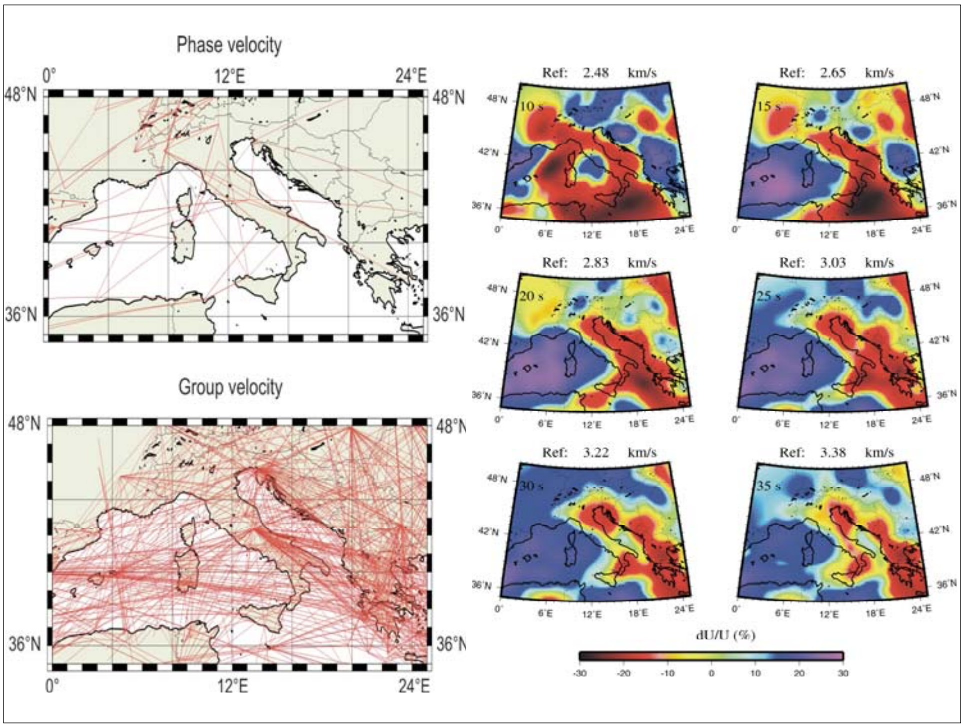

Tomography maps with superimposed cellular grid: a) group velocity, b) phase velocity

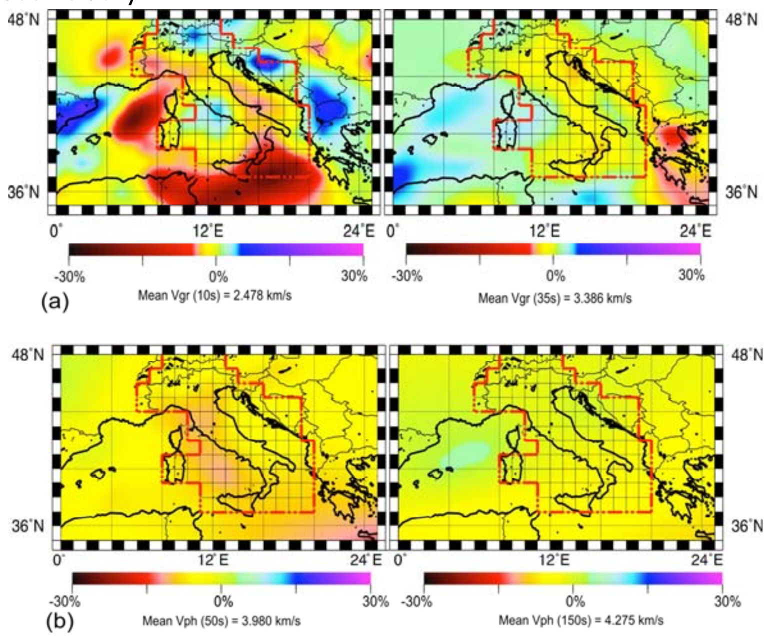

Inverse problem

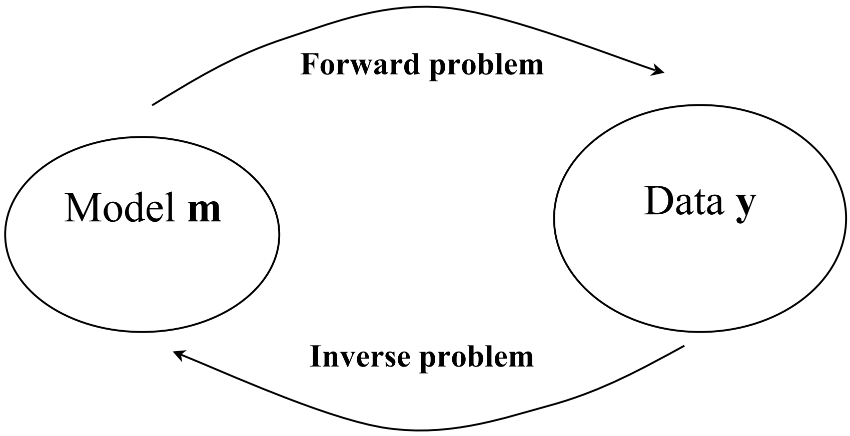

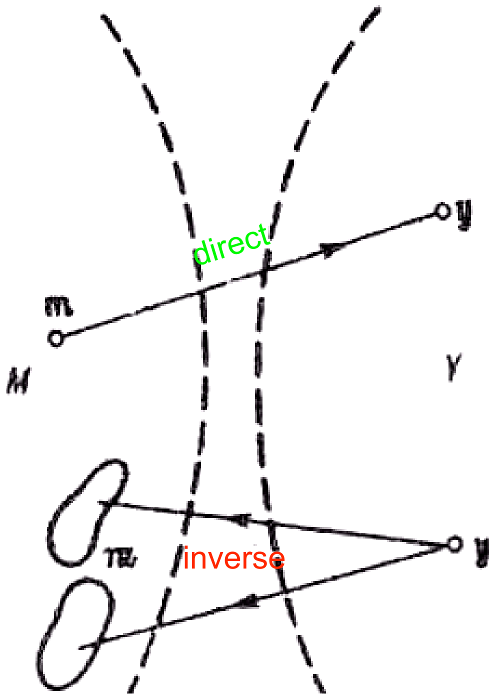

Relation between models space **M** and observations space **Y** (Yanovskaya, 2003)

Non-linear inversion

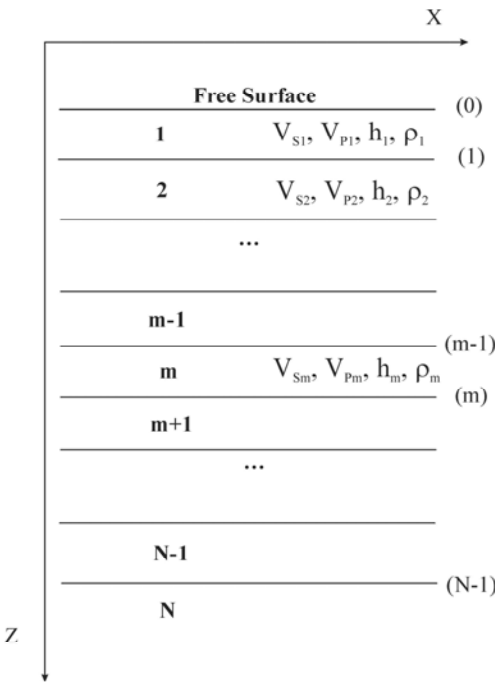

Structural model is a stack of N homogeneous isotropic layers, each one defined by compressional (V_p) and shear (V_s) wave velocities, thickness (h) and density (ρ). Boundaries between two layers are indicated with (m).

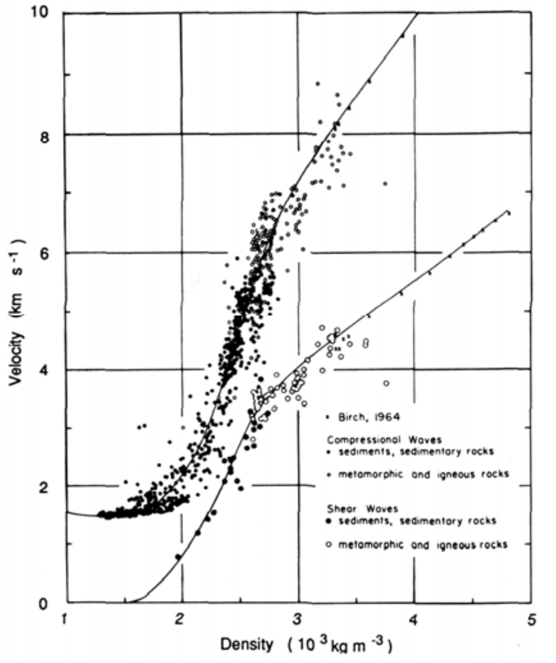

Nafe and Drake curve (e.g. Fowler, 1995; Ludwig et al., 1970) that connects seismic velocities and density.

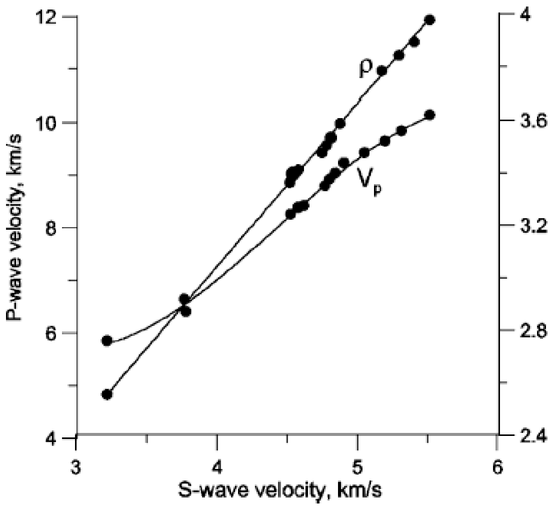

Relationship between P-wave velocity, density and S-wave velocity for PREM. Points represent the PREM (Dziewonski and Anderson, 1981) values, lines represent a possible approximation to be used in inversion studies (from Yanovskaya and Kozhevnikov, 2003).

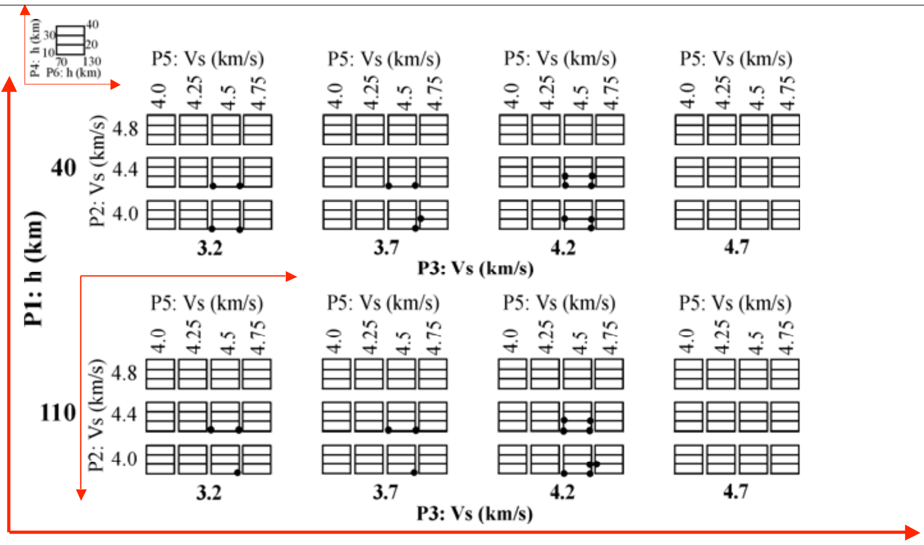

Acceptable solutions (dots) in a six-dimension model space. Thickness (h) and V_s are inverted for three layers (the parameters P1-P2, P4-P3 and P6-P5 are the three couples h-V_s for the three layers). In the main horizontal scale (bold characters) **P3 (V_s)**; in the main vertical scale (bold characters) **P1 (h)**; the horizontal and vertical scales for each composite grid are for P5 and P2 (V_s). Each little grid (see uppermost left corner) is for P4 and P6 (h).

The Resolution

A description of model variance corresponding to the data variances, in a N-dimensional parameter space, requires the specification of a large number of values. To simplify this task, it is possible to choose to list the diagonal elements of the model error matrix (i.e. the covariance matrix multiplied by σ^{-2}), which are the intercepts of the solution ellipsoid with the parameter axes Pj:

$$\left[\frac{1}{N}\sum_{i=1}^{N}\left(\frac{\partial V(T_i)}{\partial P_j}\right)^2 \sigma^{-2}(T_i)\right]^{-\frac{1}{2}} \qquad (1)$$

where $V(T_i)$ and $\sigma(T_i)$ are considered equal to $U(T_i)$ and $\sigma_U(T_i)$ for the group velocity case, or equal to $c(T_i)$ and $\sigma_c(T_i)$ for the phase velocity case, or any other relevant parameter.

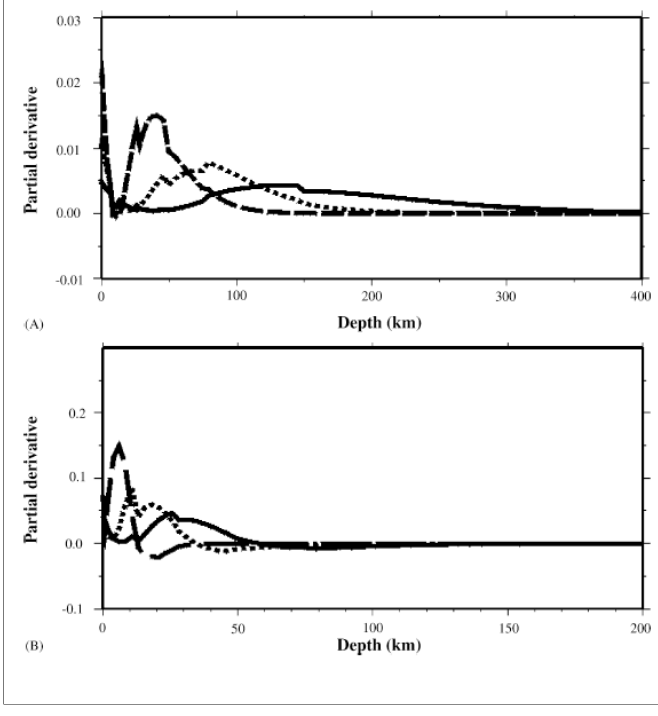

(A) Examples of partial derivatives of the phase velocity of Rayleigh waves with respect to shear-wave velocity of the fundamental mode at 100 s (solid line), 50 s (dotted line) and 30 s (dashed line).
(B) Examples of partial derivatives of the group velocity of Rayleigh waves with respect to shear-wave velocity of the fundamental mode at 30 s (solid line), 20 s (dotted line) and 10 s (dashed line).
All partial derivatives are normalized with respect to the layer thickness.

If the parameter P_j is allowed to vary by an amount δP_j from its starting value, while the others are held fixed at the starting value, then the r.m.s. difference between the exact result and the model result is:

$$\left[\frac{1}{N} \sum_{i=1}^{N} \left(\frac{\partial V(T_i)}{\partial P_j} \right)^2 \right]^{\frac{1}{2}} \delta P_j \qquad (2)$$

which can be set equal to the pre-assigned value σ.

The quantities given by (1) can be equalized to the standard deviation in the parameters P_j for the case in which all the other parameters P_i ($i \neq j$) are kept fixed at their starting values. Thus the tabulation of the items (1) does give some rough information regarding the resolution of the parameter P_j by the data set and the quantities (1) can be called the resolution, despite the fact that this definition is inconsistent with other usages in the literature.

In absence of correlation among parameters, the maximum resolution for a given model parameter, P_j, could be achieved by retaining only one datum, $V(T_i)$, specifically that for which it is satisfied the condition:

$$\mathrm{Min}\left[\left(\frac{\partial V(T_i)}{\partial P_j}\right)^{-1}\sigma(T_i)\right] \qquad (3)$$

The parameters are, in general, not independent, thus the resolution of each is poorer than the values obtained by (3) and the full problem requires the determination of the period for which the quantities δP_j are minima subject to the condition:

$$\sum_j\left(\frac{\partial V(T_i)}{\partial P_j}\right)\delta P_j = \sigma(T_i) \qquad (4)$$

In applying the hedgehog inversion, the parameterization is defined so that the parameter steps are minima, subject to the condition (4). Therefore for all the solutions of the hedgehog inversion, the step, $a_i\delta P_j$, for each parameter P_j is such that $a_i=\pm1$ or 0, at the end of the inversion. In this way each parameter step represents a satisfactory estimate of the uncertainty affecting each parameter.

The effect

of different constraints in the a priori fixed structure and

of different parameterization

TEST-1: we show that the inversion of the same phase velocity but of group velocity that differ for T≤25 s can be consistent with significantly different models, depending on the constraints imposed by the a priori knowledge, about the uppermost structure.

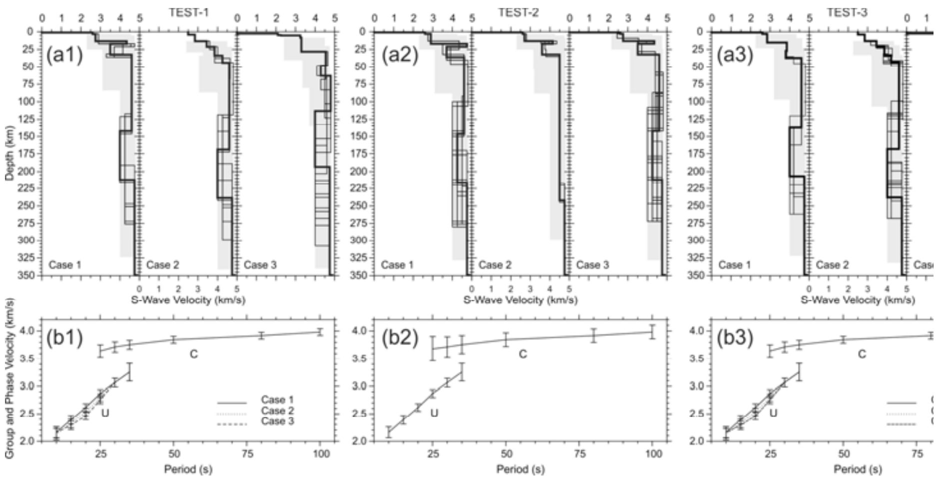

Results of tests 1, 2 and 3. (a1, a2, a3) Sets of solutions (thin lines) obtained through the non–linear inversion of the dispersion relations shown in (b1, b2, b3). The investigated parameter's spaces (grey zones) and the chosen solutions (bold lines) are shown as well. The parameterization used in the inversion is given in Tab. 4. (b1, b2, b3) Group (U) and phase (C) velocity curves used in the tests (see Tab. 3).

TEST-2: inversion of the same dispersion curves with three different parameterizations. In the three cases are inverted the thickness and velocity of:

5 layers (case-1),

4 layers (case-2) and

6 layers (case-3).

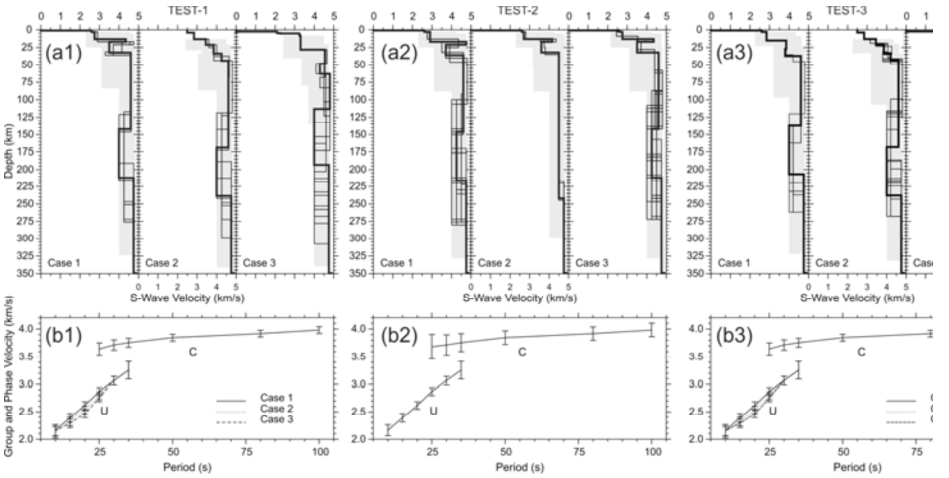

Results of tests 1, 2 and 3. (a1, a2, a3) Sets of solutions (thin lines) obtained through the non–linear inversion of the dispersion relations shown in (b1, b2, b3). The investigated parameter's spaces (grey zones) and the chosen solutions (bold lines) are shown as well. The parameterization used in the inversion is given in Tab. 4. (b1, b2, b3) Group (U) and phase (C) velocity curves used in the tests (see Tab. 3).

The parameterization does not affect the uppermost structure (a low velocity layer is present in all the cases). From the number of the obtained solutions (20, 10 and 40 respectively) and from the type of solutions obtained, 5 layers (10 parameters) is the optimum number of layers to invert in the depth interval that we are investigating.

At depth larger than 100 km the structures in case-1 and 3 have very similar trend, whilst the rough parametrization in case-2 misses a relevant feature like the mantle lvz seen in cases 1 and 3.

TEST-3: the dispersion curves and the parameterization used for the three cases are the same as in TEST-1 but starting values, variability ranges and steps of the parameters are the same for the three cases.

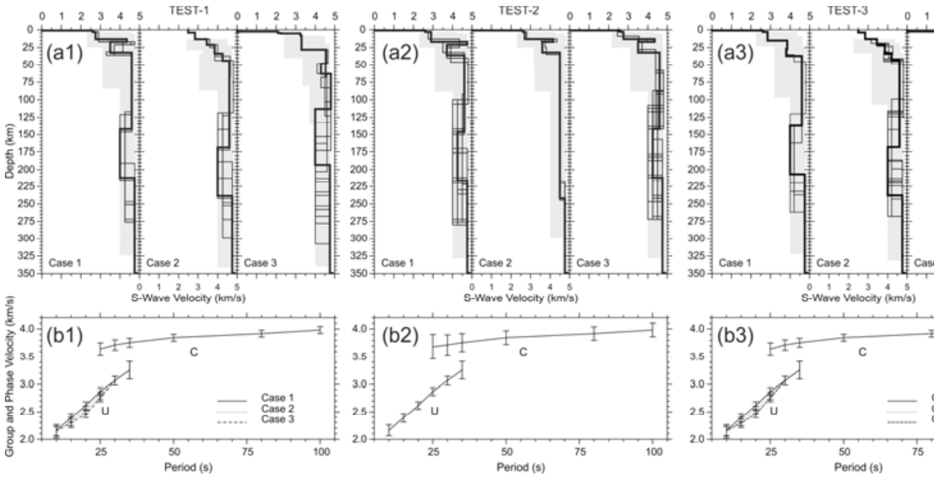

Results of tests 1, 2 and 3. (a1, a2, a3) Sets of solutions (thin lines) obtained through the non–linear inversion of the dispersion relations shown in (b1, b2, b3). The investigated parameter's spaces (grey zones) and the chosen solutions (bold lines) are shown as well. The parameterization used in the inversion is given in Tab. 4. (b1, b2, b3) Group (U) and phase (C) velocity curves used in the tests (see Tab. 3).

This test, as well as TEST-1, shows that the sets of structures are quite different also at mantle depths even if the inversion is performed for the same phase velocities and same parameterization but by slightly different group velocities and different a priori constraints at crustal level.

Furthermore, a comparison between the sets of solutions of TEST-1 and TEST-3 shows that if the result is not so different for case-2, it is different at crustal and uppermost mantle depths for cases 1 and 3. Thus, not only the number of layers inverted but also the values of the incremental step of the parameters are important, and they must be chosen accordingly to condition (4).

The choice of the representative solution

Two typical approaches: (a) choosing the 'Median Model' of all the solutions (Shapiro and Ritzwoller, 2002) as representative model; (b) choosing the model characterized by the minimum r.m.s. Other approaches are inspired by William of Occam, who wrote "it is vain to do with more what can be done with fewer" (see Russell, 1946, ch.14).

What has become known as Occam's razor has become fundamental in modern science, i.e. **hypotheses should be neither unnecessarily complicated nor unnecessarily numerous**.

Taking into account the origin of the problem (surface waves tomography – an intrinsically smoothing technique), the developed criteria of optimization consists in finding for each cell, the representative solution so that the lateral velocity gradient between neighbouring cells is minimized. One motivation for seeking smooth global models is that we want to avoid the introduction of heterogeneities that can possibly arise from a subjective choice.

Starting from the search of the representative solution in one cell (called starting cell) we look for the representative solution in all the other cells of the studied domain W, following the criteria of maximum smoothness.

The method is fast but it depends from the starting cell that can be chosen either by objective criteria, e.g. the cell where the solutions are the densest in the parameter's space, or by adequate geophysical and geological information.

Other methods of optimization, more independent from the single starting cell, have been developed based on dynamic programming method (e.g., Bryson et al., 1975).

Short description of LSO, GSO and GFO

The non-linear inversion of geophysical data in general does not yield a unique solution, but a single model representing the investigated field is preferred for an easy geological interpretation of observations. The analyzed region is constituted by a number of sub-regions where multi-valued non-linear inversion is applied, which leads to a multi-valued solution.

Therefore, combining the values of the solution in each sub-region, many acceptable models are obtained for the entire region and this complicates the geological interpretation of geophysical investigations. New developed methodologies are capable of selecting one model among all acceptable ones, satisfying different criteria of smoothness in the explored space of solutions.

(1) **Local Smoothness Optimization (LSO):** The optimized local solution is the one that is searched for, cell by cell, considering only the neighbours of the selected cell and fixing the solution as the one which minimizes the norm between such neighbours.

(2) **Global Flatness Optimization (GFO):** The optimized global solution with respect to the flatness criterion is the one with minimum global norm in-between the set $G(\Omega)$.

(3) **Global Smoothness Optimization (GSO):** The optimized global solution with respect to the smoothness criterion is the one with minimum norm among all the members of the set $\Gamma(\Omega)$.

The GSO is based on the idea of close neighbours (local smoothness) extended, in a way, to the whole study domain. The method consists of two general steps. The first step extracts a suitable subset $\Gamma(\Omega)$ from $G(\Omega)$ namely the global combination u belongs to $\Gamma(\Omega)$ if and only if

$$|u_{i,j} - u_{i\pm1,j\pm1}| = \min_{\tilde{u}\in\delta_{i\pm1,j\pm1}} (|u_{i,j} - \tilde{u}|).$$

In other words $\Gamma(\Omega)$ contains all global combinations with close neighbouring components. Then we select as the best solution in $G(\Omega)$ with respect to the smoothness criteria, the member of $\Gamma(\Omega)$ with least global norm, or we apply the flatness criteria to $\Gamma(\Omega)$ and not to the entire $G(\Omega)$.

The cellular models of the lithosphere-asthenosphere system in the Italian region

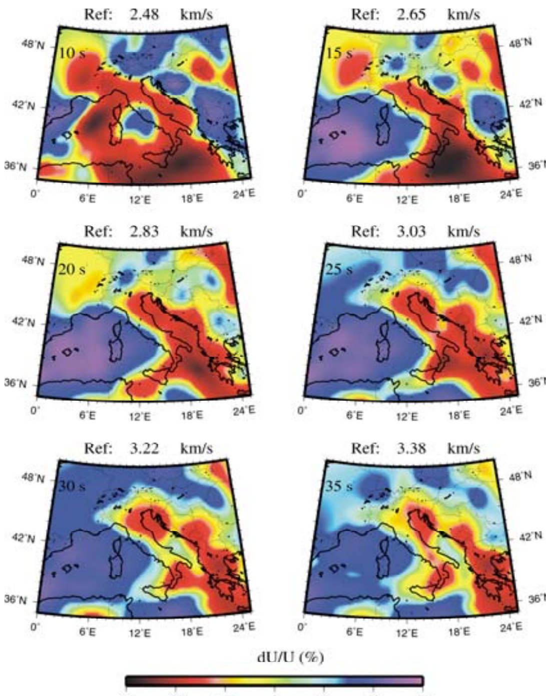

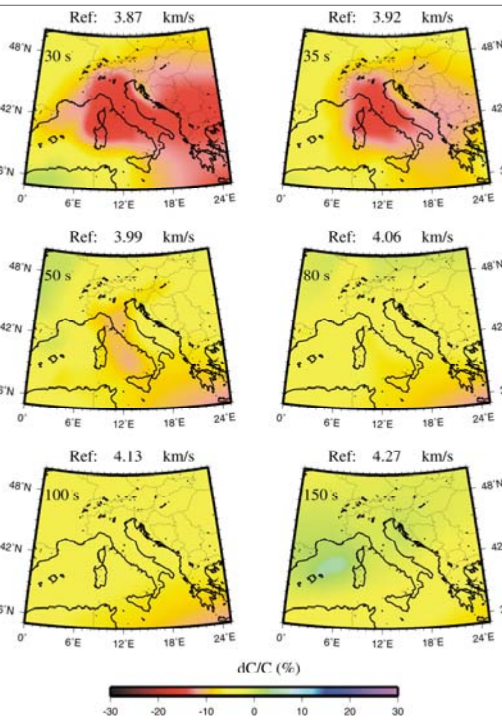

Large numbers: V_S solution choosen by LSO

Small numbers: V_S ranges

Rectangles: thickness ranges

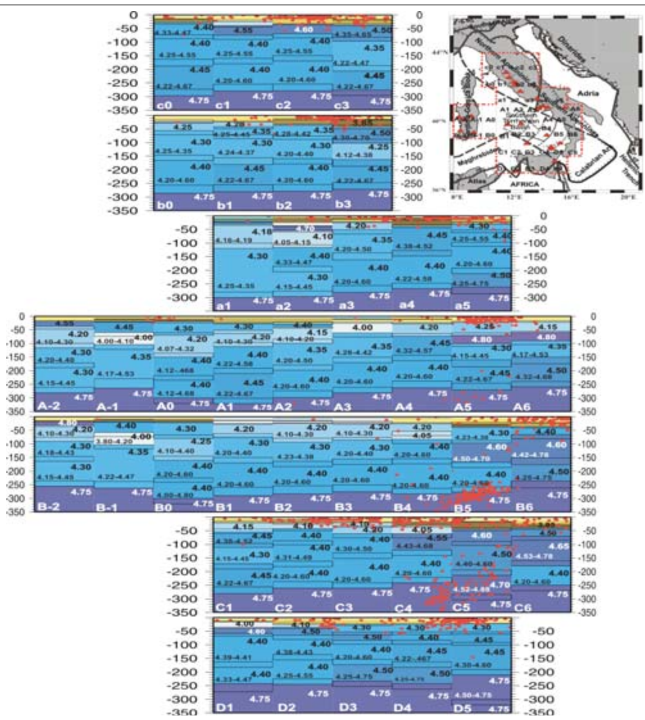

numbers: V_S solution choosen by LSO

Dashed areas: thickness ranges

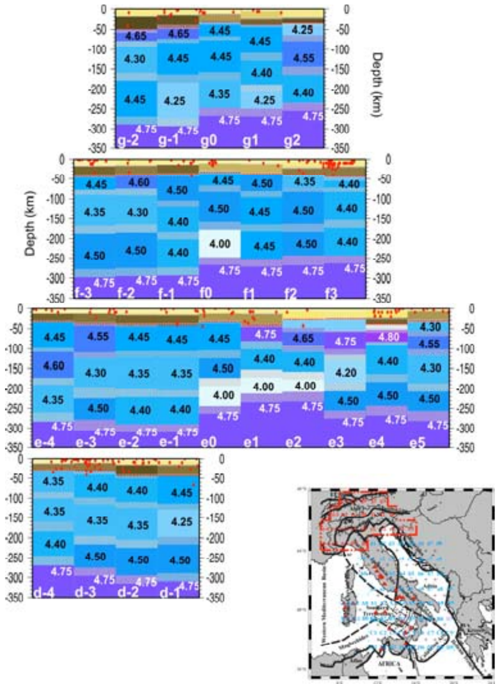

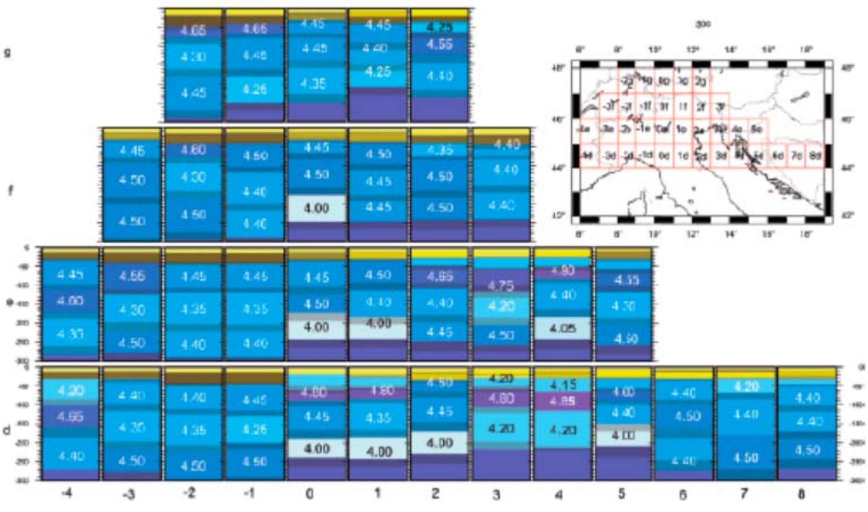

Solutions obtained by GFO, constraining solutions that are common to LSO and GSO

The lithosphere-asthenosphere system in the Mediterranean region

3D model of Vrancea

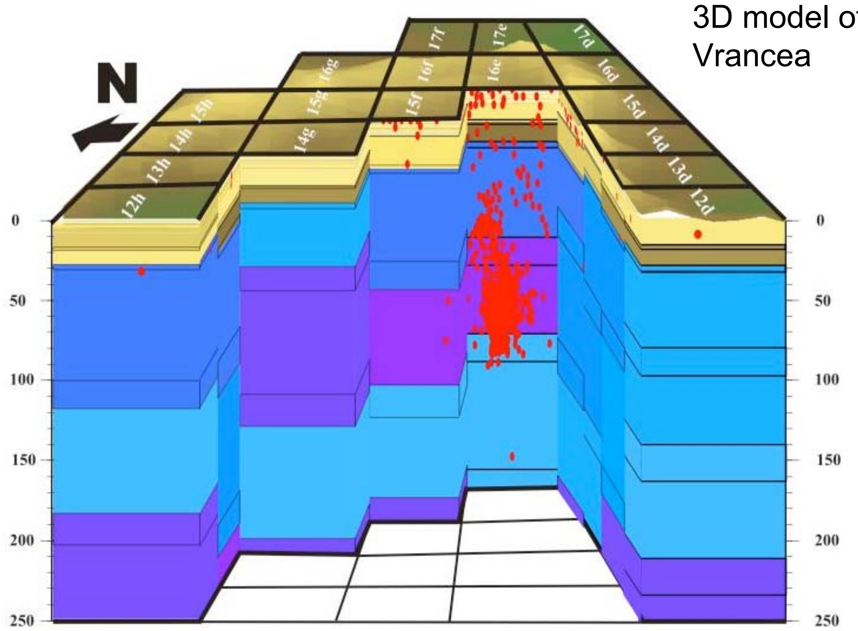

(Raykova and Panza, PEPI 2006)

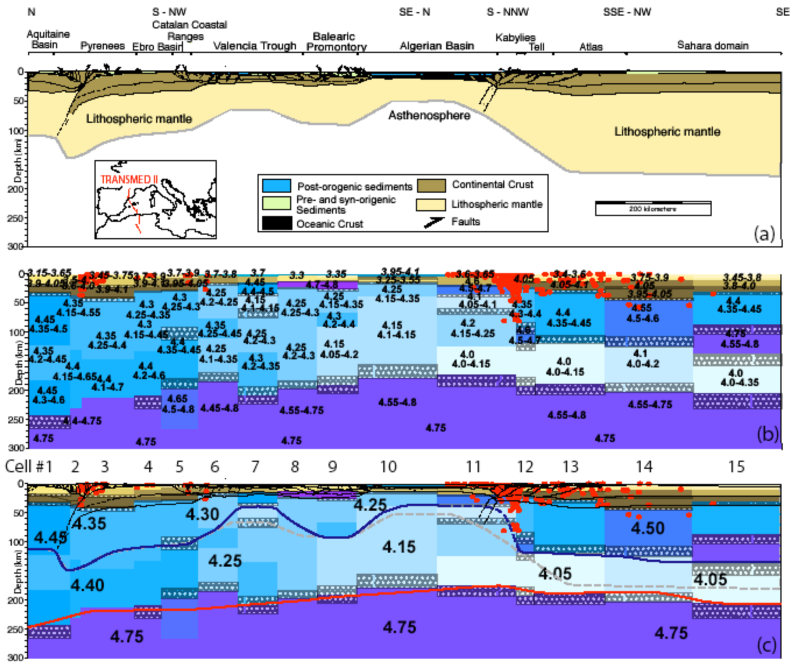
N
S - NW
SE - N
S - NNW
SSE - NW
SE
Aquitaine Basin
Pyrenees
Ebro Basin
Catalan Coastal Ranges
Valencia Trough
Balearic Promontory
Algerian Basin
Kabylies
Tell
Atlas
Sahara domain
Lithospheric mantle
Asthenosphere
Lithospheric mantle
TRANSMED II
Post-orogenic sediments
Pre- and syn-origenic Sediments
Oceanic Crust
Continental Crust
Lithospheric mantle
Faults
(a)
(b)
Cell #1 2 3 4 5 6 7 8 9 10 11 12 13 14 15
(c)

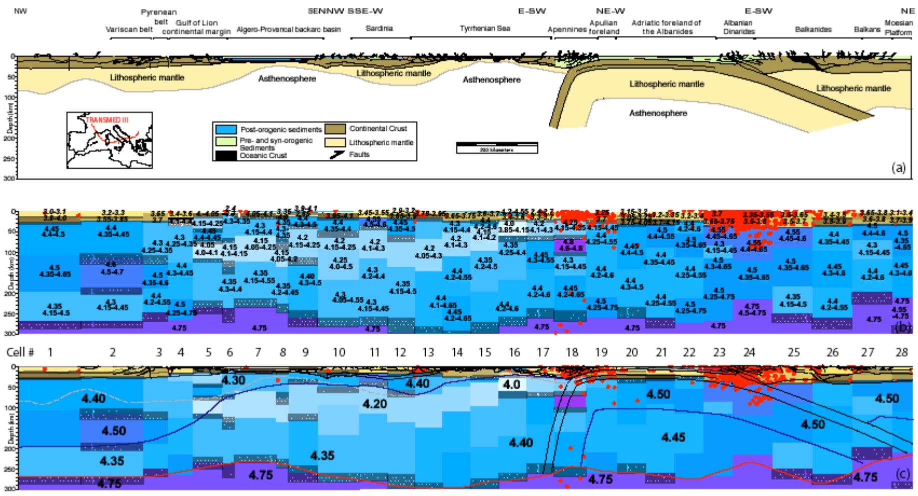
NW
NE
Variscan belt
Pyrenean belt
Gulf of Lion continental margin
Algero-Provencal backarc basin
Sardinia
Tyrrhenian Sea
Apennines
Apulian foreland
Adriatic foreland of the Albanides
Albanian Dinarides
Balkanides
Balkans
Moesian Platform
Lithospheric mantle
Asthenosphere
TRANSMED III
Post-orogenic sediments
Pre- and syn-orogenic Sediments
Oceanic Crust
Continental Crust
Lithospheric mantle
Faults
(a)
(b)
Cell # 1 2 3 4 5 6 7 8 9 10 11 12 13 14 15 16 17 18 19 20 21 22 23 24 25 26 27 28
(c)

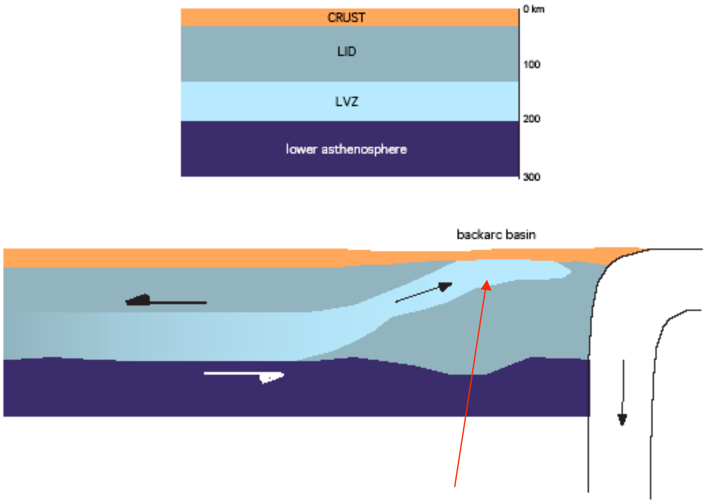

splash of mantle: volcanoes

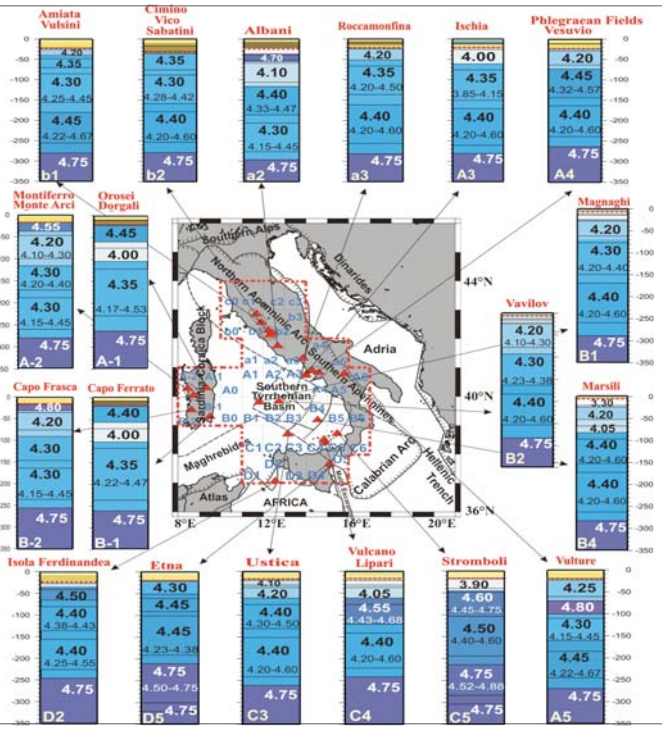

P l i o - Quaternary magmatic provinces in Italy.

Modified after Peccerillo and Panza (1999)

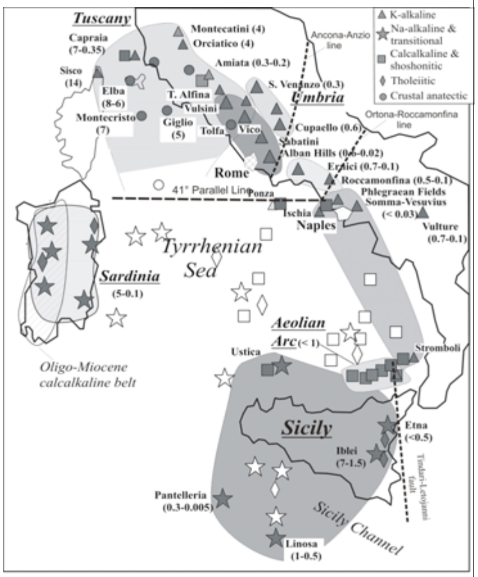

Cartoon showing the three-dimensional geodynamic scheme of the Tyrrhenian basin and bordering volcanic areas, including the subduction of the Ionian-Adria lithosphere in

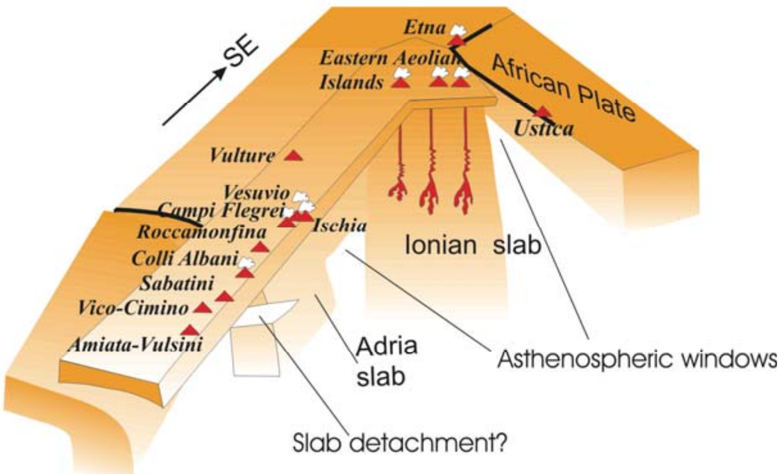

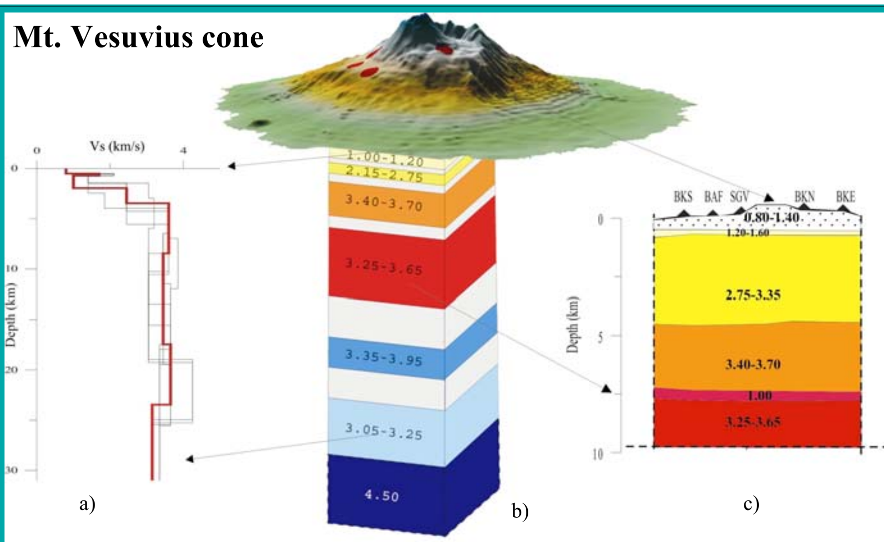

(a) Hedgehog solutions (lines) from the average Rayleigh wave group velocity dispersion curve computed, in the period range 0.3-2 s, for all stations on **Mt. Vesuvius cone** (BAF, BKN, BKS, BKE, SGV), and regional group (T=10-35s) and phase (25-100s) velocities.
(b) The chosen Vs models are shown along SE-NW-SW-NE cross-sections through Somma-Vesuvius. The grey bands indicate the boundaries between layers, that can well be transition zones in their own right, and the group of numbers indicate the ranges for V_S in km/s.
(c) Uppermost part of the chosen model, if we impose, as a priori information, the value of 1.0km/s (Auger et al., 2003), for the low velocity layer at 8km of depths (this ultralow-velocity layer is present in all solutions).

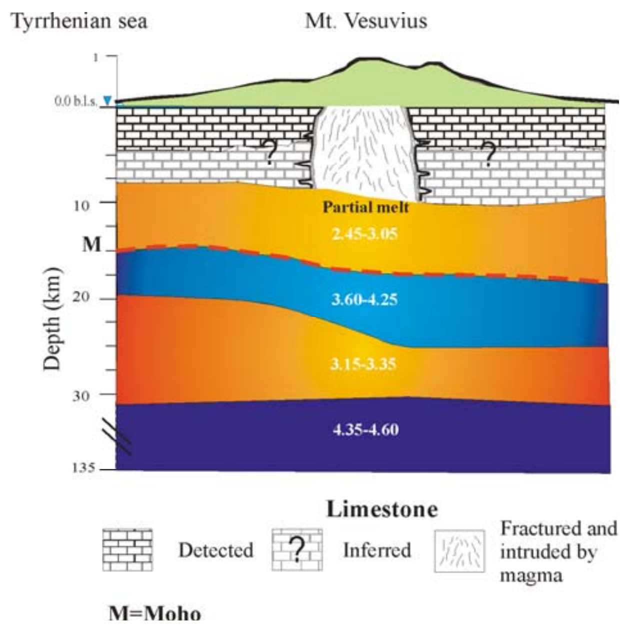

Schematic model of the crust and uppermost mantle at Mt. Vesuvius. The possible ranges of Vs are given in the figure while the uncertainty (about 1-2 km) of the thickness for each layer is omitted for clarity reasons. The Moho depth (M) is shown as dashed line.

Some special cases

The use of seismicity to identify Moho

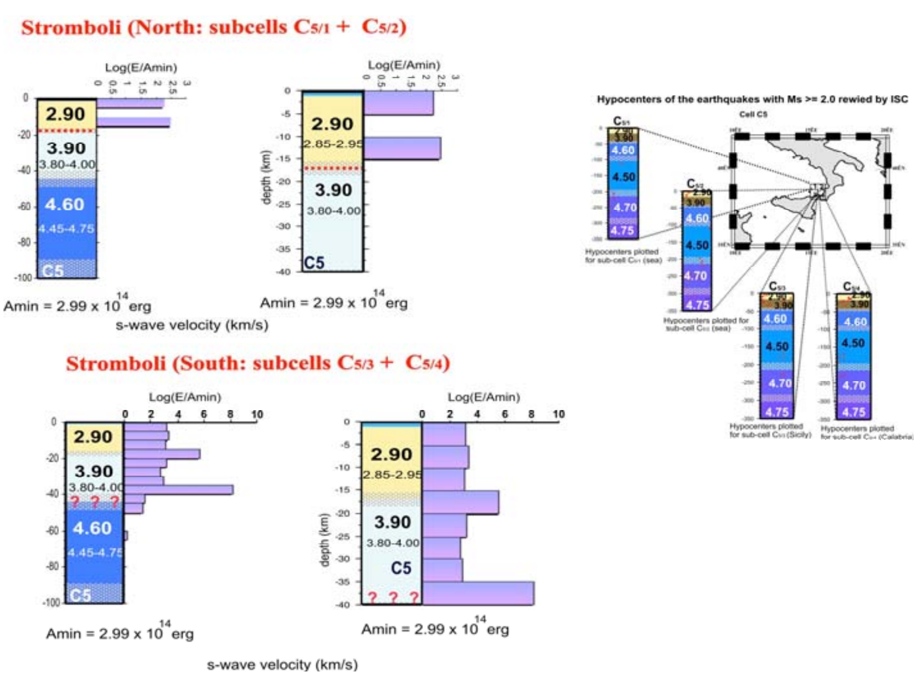

Cellular V_s structures and related logE-h distribution of earthquakes, obtained grouping hypocentres in 4-km intervals. The average V_s (km s^{-1}) and its range of variability are printed on each layer and a hatched zone outlines the range of variability of their thicknesses. Hypocentres with magnitude type specified are denoted by red dots. Hypocentres with magnitude ≥ 2.5, but of unspecified magnitude type, are denoted by purple circles. Normalized logE is shown in the right hand graph for each cell, the normalizing value $logE_{max}$ is given on the horizontal axis.

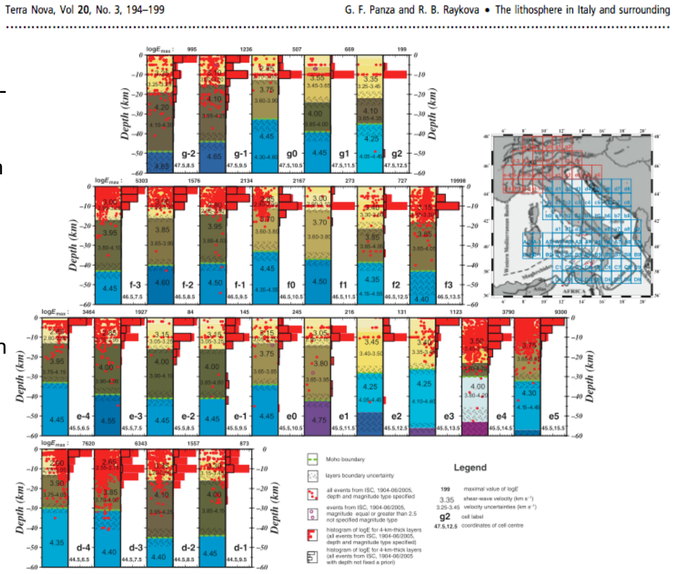

Filled red bars histogram: energy of all earthquakes from the revised ISC (2007) catalogue. Black line histogram: the energy of earthquakes for which the depth is not fixed a priori in ISC (2007). The location of each cell is shown superimposed to the structural and kinematic sketch of Italy and surrounding areas (Meletti et al., 2000).

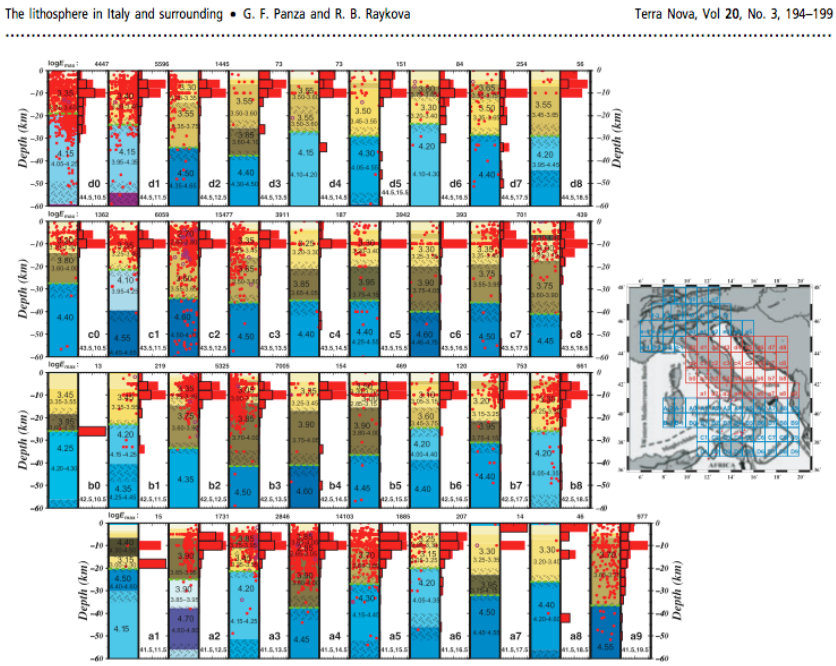

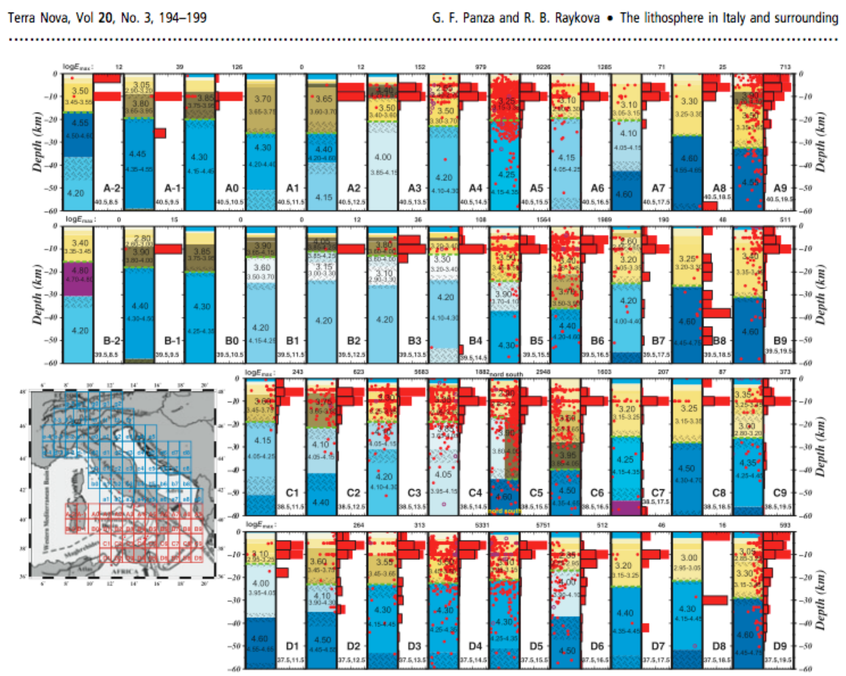

In general earthquakes are limited to the crust, but in several cells significant seismicity is observed in the uppermost upper mantle. Particularly relevant the situation in the Etna area. The earthquakes in South-eastern Sicily, named unequivocally *tectonic* or rather determined only by the release of tension associated with plate-tectonics, are also generated by local movements of the mantle from which the volcanic phenomena observed depend. These movements, which happen when the tensional state of crust varies substantially, may determine the fragile deformation of the latter and therefore may trigger earthquakes, even with notable energy.

The end